JACS
JOURNAL OF THE AMERICAN CHEMICAL SOCIETY
Article
pubs.acs.org/JACS

Multifaceted Regioregular Oligo(thieno[3,4-*b*]thiophene)s Enabled by Tunable Quinoidization and Reduced Energy Band Gap

Feng Liu,[†] Guzmán L. Espejo,[‡] Shuhai Qiu,[†] María Moreno Oliva,[‡,§] João Pina,[§] J. Sérgio Seixas de Melo,[§] Juan Casado,*[,‡] and Xiaozhang Zhu*[,†]

[†]Beijing National Laboratory for Molecular Sciences, CAS Key Laboratory of Organic Solids, Institute of Chemistry, Chinese Academy of Sciences, Beijing, 100190, P. R. China

[‡]Department of Physical Chemistry, University of Málaga, Campus de Teatinos s/n, Málaga, 29071, Spain

[§]Coimbra Chemistry Centre, Department of Chemistry, University of Coimbra, Rua Larga Coimbra, 3004-535, Portugal

Supporting Information

ABSTRACT: Thiophene-based materials have occupied a crucial position in the development of organic electronics. However, the energy band gaps of oligo- and polythiophenes are difficult to modulate without resorting to push−pull electronic effects. We describe herein a new series of monodisperse oligo(thieno[3,4-*b*]thiophene) derivatives with well-defined regioregular structures synthesized efficiently by direct C−H arylation. These compounds show a unique palette of colors and amphoteric redox properties with widely tunable energy band gaps. The capacity to stabilize both cations and anions results in both anodic and cathodic electrochromism. Under excitation, these compounds can produce photoionized states able to interconvert into neutral triplet or form these through singlet exciton fission or intersystem crossing. These features arise from a progressive increase in quinoidization on a fully planar platform making the largest effective conjugation length among hetero-oligomers. Oligo(thieno[3,4-*b*]thiophene)s might represent the more distinctive family of oligothiophenes of this decade.

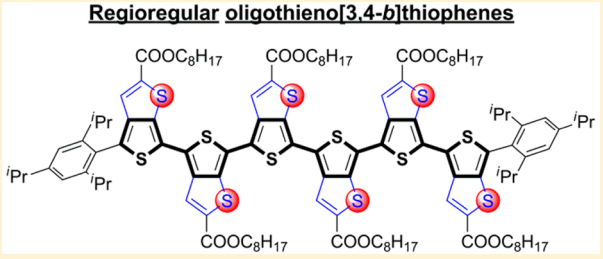

INTRODUCTION

The energy band gap of organic π-conjugated materials is a primary characteristic that can be adjusted, e.g., by molecular engineering, to optimize a material for organic electronic applications.[1] Since Wudl et al. first synthesized poly(isothianaphthene) (**PITN**) with a intriguingly small highest occupied molecular orbital (HOMO)−lowest unoccupied molecular orbital (LUMO) gap (HLG) of 1.0 eV,[2] the enhancement of quinoid resonance by peripheral modification has become a powerful strategy for the development of organic materials with narrow HLG (Figure 1),[3] which is a well-established prerequisite for obtaining high-performance organic-based electronic and optoelectronic devices.[4] By analogy to **PITN**, poly(thieno[3,4-*c*]thiophene) (**PT*c*T**)[5] was also predicted to be a member of the group of small-HLG compounds because of its similar quinoidization effects. However, both **PITN** and **PT*c*T** suffer from steric S···H repulsions and coplanarity deviations, which deteriorate the HLG. The isomeric polymer of **PT*c*T**, regioregular poly(thieno[3,4-*b*]thiophene) (**PT*b*T**), avoids such steric crowding and hence favors full backbone planarization. Furthermore, as for **PT*c*T**, the balance of aromaticity between the peripheral thiophene and oligothienyl thiophene might also impart a quinoidal synergy to the polythiophene chain. The intrinsic difficulties of preparing thieno[3,4-*b*]thiophene (**T*b*T**) derivatives relate, among other factors, to defining the regioregularity of the final products, which may explain why such compounds have received relatively little attention. Recently, **T*b*T** has been utilized as a key building block for the construction of small HLG homopolymers with random regioselectivity.[6] Yu et al.[7] have also taken advantage of the quinoid-enhancing features of the **T*b*T** unit to develop one of the most successful p-type low-HLG copolymer materials, **PTB7**, for organic photovoltaic applications.

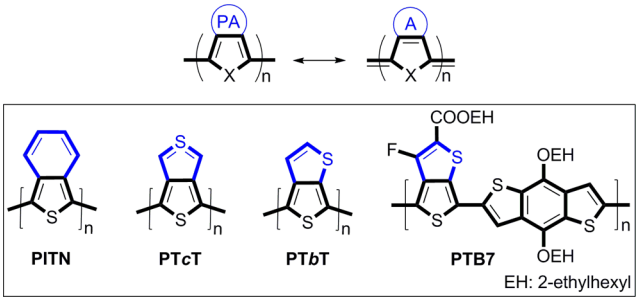

Figure 1. Top: Aromatic (left) and quinoid (right) resonance structures in conjugated oligomers and polymers. PA: pro-aromatic; A: aromatic; X: heteroatom. Bottom: Basic chemical structures of the main polymers mentioned in the text.

Received: June 13, 2015
Published: July 17, 2015

DOI: 10.1021/jacs.5b05940
J. Am. Chem. Soc. 2015, 137, 10357−10366

Scheme 1. Synthesis of Key rr-OT*b*T Precursors[a]

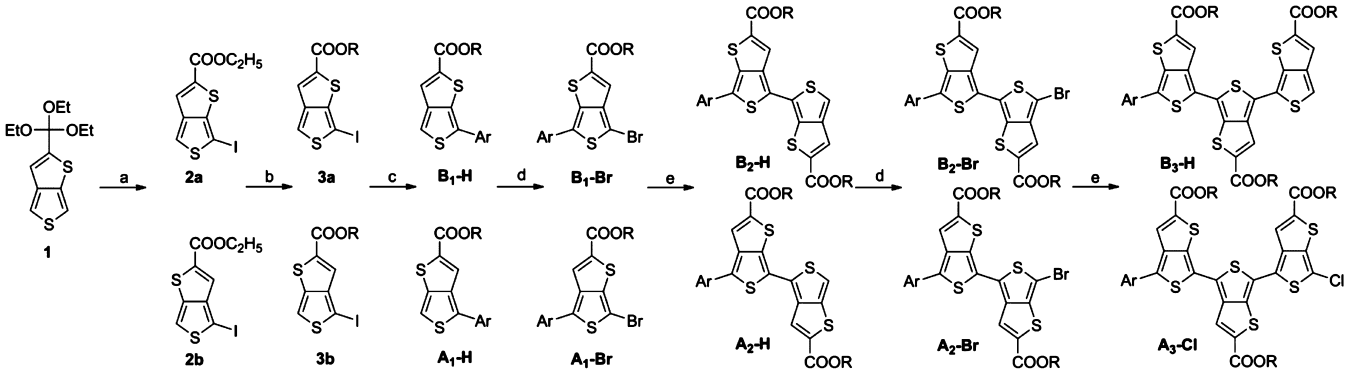

[a]Reagents and conditions: (a) (i) *n*-BuLi/*n*-hexane, THF, −78 °C; (ii) HCl; (b) (i) LiOH, EtOH, reflux; (ii) 1-octanol, *N*,*N*′-dicyclohexylcarbodiimide (DCC), 4-dimethylaminopyridine (DMAP), CH_2Cl_2, rt; (c) (2,4,6-triisopropylphenyl)boronic acid, $Pd(PPh_3)_2Cl_2$, Cs_2CO_3, dioxane, 80 °C; (d) *N*-bromosuccinimide (NBS), $CHCl_3$, under dark, rt; (e) Octyl 6-(tributylstannyl)thieno[3,4-*b*]thiophene-2-carboxylate, octyl 4-(tributylstannyl)thieno[3,4-*b*]thiophene-2-carboxylate, or octyl 6-chloro-4-(tributylstannyl)thieno[3,4-*b*]thiophene-2-carboxylate, $Pd(PPh_3)_4$, toluene, 100 °C.

The challenging synthesis[8] of regioregular thieno[3,4-*b*]-thiophene oligomers has meant that the preparation of a complete series of such compounds has not yet been realized. Nevertheless, series of oligomers of increasing size are highly valuable in organic electronics because an examination of such sets can allow the precise electronic and molecular properties of an infinite polymer (oligomer approach),[9] i.e., free of any chemical or structural defect to be inferred. Furthermore, such studies can reveal structure property relationships, which are needed to develop improved chemical designs. With access to oligo(thieno[3,4-*b*]thiophene) derivatives, the intrinsic **T*b*T** quinoidization and coplanarity effects, the extent of conjugation length, the dependence of the electronic and optical properties on size, and the influence of HOMO−LUMO gaps can be clarified for the relatively unexplored poly(thieno[3,4-*b*]-thiophene) family. Such developments could lead to promising new, next-generation organic materials.

We report herein for the first time the synthesis of a series of regioregular oligo((*n*-octyloxy)carbonyl thieno[3,4-*b*]-thiophene) (**rr-OT*b*T**) derivatives with well-defined planar structures. The synthesis was achieved by overcoming two key obstacles: (1) control of regioregularity, which is inherently challenging because of the unsymmetrical nature of **T*b*T**, and (2) the issue of stability, which is ascribed to the quinoidal shape and the propensity of such compounds to form reactive biradicaloid species.[10] The **rr-OT*b*T** derivatives exhibit a surprisingly broad spectrum of absorptions ranging from the UV−vis to the near-infrared (NIR) region, with an extremely long effective conjugation length of approximately 30 thiophene repeating units. The HLG continuously narrows with increasing size, and a small band gap for longer oligomers and polymers would clearly be expected. A concomitant and significant increment of ground electronic state quinoidization (π-electron delocalization), which does not saturate at the hexamer, is found. Quinoidization lies at the origin of both the amphoteric redox and the unique photophysical properties. A study of the redox species reveals an unprecedented equal stabilization/delocalization of both positive and negative excess charges of the **T*b*T** platforms, with both being accompanied by a distinct electrochromism consisting of an exchange between colorful neutral and colorless redox species, which, combined, constitute strongly absorbing NIR dyes.

RESULTS AND DISCUSSION

Synthesis of rr-OT*b*Ts. To address the stability and regioregularity issues, we protected the two terminals of **rr-OT*b*T** derivatives with bulky 2,4,6-triisopropylphenyl substituents and prepared octyl 6-iodothieno[3,4-*b*]thiophene-2-carboxylate (**3a**) and octyl 4-iodothieno[3,4-*b*]thiophene-2-carboxylate (**3b**) as key precursors. The synthesis of some key precursors is indicated in Scheme 1. By deprotonation of 2-(triethoxymethyl)thieno[3,4-*b*]thiophene (**1**) with *n*-BuLi, followed by iodination with diiodoethane and deprotection with dilute hydrochloric acid, compounds **2a** and **2b** were obtained, which could be separated by silica-gel column chromatography in 60 and 20% yields, respectively. Compounds **2a** and **2b** were then hydrolyzed, followed by Steglich esterification to give *n*-octyl-substituted compounds **3a** and **3b** for the synthesis of **rr-OT*b*T** derivatives with adequate solubility. $\mathbf{A_1}$-H and $\mathbf{B_1}$-H were then obtained by Suzuki coupling between (2,4,6-triisopropylphenyl)boronic acid and compounds **3b** and **3a** in 93 and 89% yields, respectively. Bromination of compounds **3b** and **3a** with *N*-bromosuccinimide (NBS) in the dark afforded $\mathbf{A_1}$-Br and $\mathbf{B_1}$-Br in 83 and 90% yields, respectively. Stille couplings between $\mathbf{A_1}$-Br or $\mathbf{B_1}$-Br and octyl 4-(tributylstannyl)thieno[3,4-*b*]thiophene-2-carboxylate or octyl 6-(tributylstannyl)thieno[3,4-*b*]thiophene-2-carboxylate gave $\mathbf{A_2}$-H or $\mathbf{B_2}$-H in 58 and 50% yields, respectively. Further bromination of compounds $\mathbf{A_2}$-H and $\mathbf{B_2}$-H was difficult because of the relative low stability of $\mathbf{A_2}$-Br and $\mathbf{B_2}$-Br. A considerable amount of $\mathbf{B_2}$-Br oligomerized during silica-gel chromatography, which resulted in a low yield of 30%; however, $\mathbf{A_2}$-Br showed better stability and could be obtained in 82% yield. $\mathbf{A_3}$-Cl and $\mathbf{B_3}$-H were synthesized by Stille coupling between $\mathbf{A_2}$-Br or $\mathbf{B_2}$-Br and octyl 6-chloro-4-(tributylstannyl)-thieno[3,4-*b*]thiophene-2-carboxylate or octyl 6-(tributylstannyl)thieno[3,4-*b*]thiophene-2-carboxylate. The enhanced quinoid resonance (see below) meant that bromination of $\mathbf{A_3}$-H or $\mathbf{B_3}$-H was not possible. The last precursor, $\mathbf{A_4}$-H, was synthesized from $\mathbf{A_3}$-Cl and octyl 4-(tributylstannyl)-thieno[3,4-*b*]thiophene-2-carboxylate by Stille-type cross-coupling involving C−Cl activation.

We found that Pd-catalyzed direct C−H arylation[11] is appropriate for the synthesis of **rr-OT*b*T** derivatives, because this approach avoids the tedious functionalization of **rr-OT*b*T**

DOI: 10.1021/jacs.5b05940
J. Am. Chem. Soc. 2015, 137, 10357−10366

precursors (Scheme 2). The direct arylation of B_1-H with A_1-Br afforded **rr-2T*b*T** in low yield (8%); however, the product

Scheme 2. Synthesis of Regioregular rr-OT*b*Ts by Direct C−H Arylation

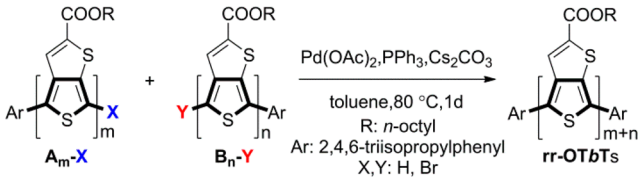

was synthesized from A_2-Br and (2,4,6- triisopropylphenyl)bor onic acid in high yield (86%). The remaining oligomers, **rr-3T*b*T**−**rr-6T*b*T**, could be synthesized through direct C−H arylation in moderate yields (50−60%). Regioregular poly(((*n*-octyloxy)carbonyl)thieno[3,4-*b*]thiophene) (**rr-PT*b*T**) was synthesized from octyl 6-chloro-4-(tributylstannyl)thieno[3,4-*b*]thiophene-2-carboxylate as a black solid in 90% yield by Stille polymerization. The **rr-OT*b*T** derivatives are white (monomer), yellow (dimer), purple-red (trimer), dark-blue (tetramer) to black (pentamer and hexamer) solids. All oligomers were unambiguously characterized by conventional analytical methods (see the Supporting Information, parts S1/S2 and Figure S1).

Photophysical and Electrochemical Properties. The light absorption range of **rr-OT*b*T** derivatives (Figure 2) covers

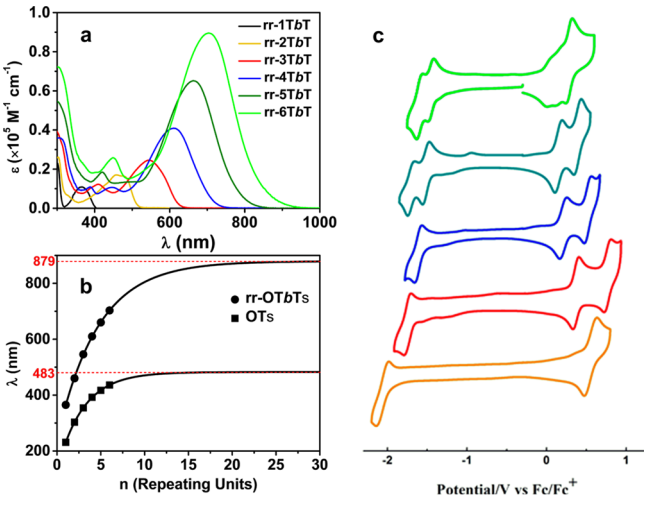

Figure 2. (a) UV−vis-NIR absorption spectra. (b) Representation of the λ_{max} of the electronic absorption spectra versus n = 1−6 for the **rr-OT*b*Ts** and **OTs** oligothiophene series together the exponential fits. (c) Cyclic voltammograms of **rr-OT*b*T** in dichloromethane. Electronic absorption spectra and cyclic voltammetries are recorded in solution.

the UV−vis to NIR region from 366 nm (**rr-1T*b*T**) to 703 nm (**rr-6T*b*T**) with very high absorption coefficients (Table 1). This contrasts with conventional oligothiophenes (**OT**s), which exhibit maximum absorption saturation below 500 nm.[12] According to Meier's equation,[13] the effective conjugation length of **rr-OT*b*T** derivatives is determined to be 30 units, which is much larger than that of **OT** (20 units).[14] The maximum absorption of the infinite polymer is estimated to be 879 nm, which is comparable to the experimentally determined value for **rr-PT*b*T** of 960 nm (Figure S2). The fluorescence quantum yield (Φ) of **rr-1T*b*T** was 71%, whereas the value for **rr-2T*b*T**−**rr-4T*b*T** was 2% (Figure S3). For **rr-3T*b*T**, picosecond-time-resolved emission was obtained, and the signal was properly fitted to a double-exponential law with decay times of 11 and 132 ps (Figure S4).[15]

The phosphorescence spectrum was obtained for **rr-1T*b*T** (Figure S5), which revealed efficient intersystem crossing (ISC)[16] for the **T*b*T** configuration because of the accumulation of heavy sulfur atoms and the quinoidal character of the singlet ground electronic state (see below). The Stokes shifts of **rr-OT*b*T** derivatives are smaller than those of **OT** derivatives and oligofurans;[17] e.g., 0.31 eV (**rr-4T*b*T**) vs 0.57 eV (**4T**) and 0.41 eV (**4F**), suggesting the rigidity of the molecular structures of **rr-OT*b*T**. UV−vis excitation spectra at 77 K (liquid N_2, see Figure S6) reveal a poor resolution of the vibronic shape, which is consistent with a rigid structure already existing at room temperature. From **rr-2T*b*T**, amphoteric electrochemical properties are observed with either one or two reversible anodic and cathodic redox processes, depending on the size. Accordingly, the HOMO energy levels increase from −5.83 eV (**rr-1T*b*T**, Figure S7) to −4.85 eV (**rr-6T*b*T**), and the LUMO energy levels decrease from −2.77 eV (**rr-2T*b*T**) to −3.37 eV (**rr-6T*b*T**) continuously covering the Fermi-level energy spectrum of the most common electrodes and relevant substrates (TiO_2 and perovskites) (see Figures S8 and S9 for the experimental and theoretical HOMO and LUMO values).

Orbital, Nucleus-Independent Chemical Shift (NICS), and Molecular Geometry Analysis. The orbital structure of the rr-**OT*b*T** derivatives obtained from the constituent parts provides insights into the effects of electronic synergy and its implications for the energy gap. The main molecular orbitals of **rr-1T*b*T**, shown in Figure 3, result from a combination of the HOMOs of thiophene and of a 2-carboxylate thioethylenic unit (their symmetric and antisymmetric combinations give rise to the HOMO and HOMO−3 orbitals of **rr-1T*b*T**) and of their LUMOs (these combinations give rise to the LUMO and LUMO+1 of **rr-1T*b*T**), yielding a significant HLG contraction and revealing the synergy effect of ring fusion. In particular, the destabilization of the HOMO in **rr-1T*b*T** from thiophene by approximately +0.5 eV highlights the significant increase in the contribution of the quinoidal canonical form to the oligothienyl thiophene. This remarkable interfragment HOMO-with-HOMO/LUMO-with-LUMO splitting in the monomer is a highly desirable property for attaining low band gap oligomers and polymers (conversely HOMO-with-LUMO combinations also produce reduced HLG but with charge transfer character). Here, ring condensation in **T*b*T** gives rise to destabilized frontier π-orbitals that favor inter-ring electron delocalization and quinoidization.

From **rr-1T*b*T** to **rr-6T*b*T**, the HLG is progressively narrowed as the HOMO energy changes from −6.09 eV in **rr-1T*b*T** to −5.03 eV in **rr-6T*b*T** (see Figures S8−S9); this is another indication of the increasing participation of the quinoidal form in the stabilization of the ground electronic state of the **rr-OT*b*T** derivatives with increasing size. This interpretation of the electronic structure of the **rr-OT*b*T** derivatives is consistent with the NICS values (see Table S2)[18] for the two classes of thiophenes of the **T*b*T** units of the six oligomers. NICS for the oligothienyl thiophenes (i.e., −13.02 ppm in **rr-1T*b*T** and −10.53/−9.21/−11.13 ppm in **rr-3T*b*T** for rings: A/B/C in Figure 4a) are always more aromatic than those of the lateral 2-carboxylate thiophenes (−6.65 ppm in **rr-1T*b*T** and −6.50/−7.23/−6.96 ppm in **rr-3T*b*T** for rings G/H/I, respectively, in Figure 4a), delineating a NICS gradient or

DOI: 10.1021/jacs.5b05940
J. Am. Chem. Soc. 2015, 137, 10357−10366

Table 1. Photophysical and Electrochemical Data for Regiogular Oligo(thieno[3,4-*b*]thiophene)s[a]

	λ_{abs} (nm)	$\varepsilon_{max} \times 10^{-4}$ (M^{-1} cm^{-1})	λ_{em} (nm)	Φ[b]	Stokes shift (eV)	$E_{ox}^{1/2}$[c] (V)	HOMO[d] (eV)	$E_{red}^{1/2}$[c] (V)	LUMO[d] (eV)	E_g^{CV} (eV)	E_g^{opt}[e] (eV)
rr-1T*b*T	366	1.11	445	71%	0.60	1.03	−5.83	–	–	–	3.10
rr-2T*b*T	455, 480	1.68	525	2.4%	0.33	0.55	−5.35	−2.03	−2.77	2.58	2.41
rr-3T*b*T	545	2.48	634	2.4%	0.32	0.35, 0.75	−5.15	−1.77	−3.03	2.12	1.98
rr-4T*b*T	612	4.09	724	1.9%	0.31	0.23, 0.50	−5.03	−1.59	−3.21	1.82	1.74
rr-5T*b*T	663	6.51	–	–	–	0.16, 0.39	−4.96	−1.49, −1.70	−3.31	1.65	1.59
rr-6T*b*T	703	8.95	–	–	–	0.03, 0.15, 0.28	−4.83	−1.43, −1.61	−3.37	1.46	1.48

[a]Measured in dichloromethane. [b]Fluorescence quantum yield was determined by absolute method. [c]CV on a carbon electrode with *n*-Bu_4NClO_4 in dichloromethane (0.1 M, vs Fc^+/Fc). [d]The HOMO and LUMO energy levels were determined by HOMO = −(4.80 + $E_{ox}^{1/2}$), LUMO = −(4.80 + $E_{red}^{1/2}$). [e]$E_g^{opt} = 1240/\lambda_{onset}$ (eV).

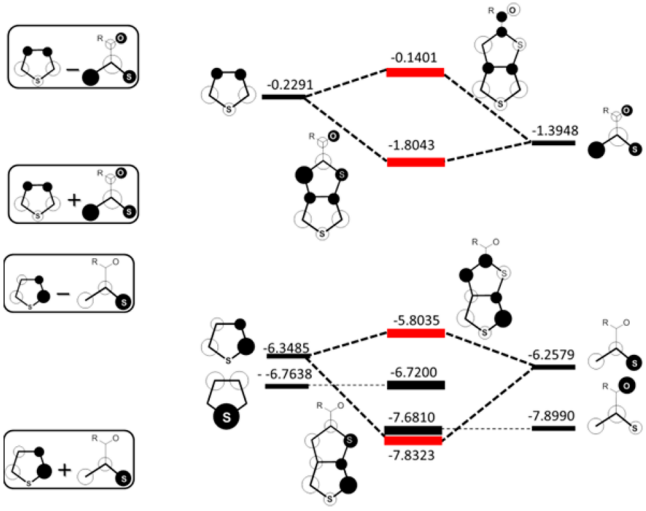

Figure 3. B3LYP/6-31G** frontier molecular orbital energies and atomic compositions of **rr-1T*b*T** as generated by a combination of their thiophene and 2-carboxylate thioethylenic fragments.

aromatic/quinoidal competition between the two types of fused thiophenes. These differences in NICS remain constant in the **rr-OT*b*T** series, which demonstrates that there is a continuity in the synergistic effect as a function of size (therefore saturation is not achieved). This contrasts with the series of unsubstituted **OT**s for which the NICS values for the central thiophenes become progressively quinoidal (−9.84 and −8.00 ppm in the outer and central rings of 3T, respectively).

The ground-state molecular structures of **rr-OT*b*T**s, shown in Figure 4b, were investigated theoretically. The results reveal two main tendencies. On one hand, the inter-ring dihedral angles between successive thiophenes are close to 180° (*anti*-planar), independent of the size, which indicates the absence of interunit steric congestion. We have successfully resolved the X-ray structure of a parent molecule of **rr-2T*b*T** (without terminal 2,4,6-triisopropylphenyl groups), and the results revealed an all-*anti* configuration of the two **T*b*T** units with a full coplanar configuration (see Figure S10). With planar conformation as the most stable geometry, the energy barrier calculated for the rotation around these inter-ring angles is always higher for **rr-OT*b*T**s than for **OT**s (Figure 4c); the lowest energy conformer for the latter is distorted, with inter-ring dihedral angles of 20–30°.[19] As noted above, the destabilized π-orbitals of **T*b*T** favor maximal inter-ring π-electron delocalization, which is nicely corroborated by analysis of the calculated bond lengths (Figure 4b). As a typical example, the geometry of **rr-6T*b*T** is compared with that of **6T**. The thiophene aromatic C═C/C−$C_{intra\text{-}ring}$ and C−$C_{inter\text{-}ring}$ bonds in the former are significantly longer/shorter than those of the latter. Indeed, the C═C bond lengths in **rr-6T*b*T** are actually similar to the intraring C−C bonds lengths of **6T**. Furthermore, the inter-ring C−C bonds of **rr-6T*b*T** are shortened with respect to those of **6T**; for instance, the average inter-ring C−C bond length of **rr-6T*b*T** is 1.429 vs 1.439 Å in **6T**. The bond-length alternation parameter (BLA) steadily decreases from **rr-1T*b*T** to **rr-6T*b*T**, highlighting the concomitant evolution of the C═C/C−C alternating bonds toward a more quinoidized or more π-conjugated path.

This description of the theoretical geometries, which is in line with backbone quinoidization, is supported by the experimental Raman spectra. Raman spectroscopy is a valuable tool with which to probe π-electron delocalization in the ground electronic state of conjugated molecules.[20] The FT-Raman spectra of **rr-OT*b*T**s, shown in Figure 4d, are characterized by a main Raman band attributed to the well-known effective conjugation coordinate (ECC) vibrational mode. The magnitude of the downshift of this frequency with extension of the chain is closely correlated with the extent of π-electron quinoidization in the ground electronic state. In **OT**s, the change in the frequency of the ECC band from the smaller members to the hexamer is approximately 20 cm^{-1},[21] showing a frequency plateau from **4T** to **6T** and longer, which is related to a saturation of π-electron delocalization. The ECC Raman mode of **rr-OT*b*T** derivatives downshift progressively on going from **rr-1T*b*T** to **rr-6T*b*T**, displaying a total variation, without a frequency plateau, of approximately 100 cm^{-1}. Further downshift with chain elongation beyond the hexamer is expected; in fact, for the **rr-PT*b*T** polymer, the ECC Raman mode is approximately 1360 cm^{-1} (see Figure S11). This approximately 100 cm^{-1} change results from the transformation of the **OT** aromatic core into a situation with reduced BLA and enhanced quinoidization and is in line with the orbital and molecular structural description described above. The rigidity/planarization imparted by the reinforced inter-ring C−C bonds leads to minimal changes to the excitation/absorption spectra in solution upon cooling, given that a repopulation toward the lowest energy conformer at lower temperatures, as observed in **OT** and many other flexible **OT**s,[22] does not occur.

DOI: 10.1021/jacs.5b05940
J. Am. Chem. Soc. 2015, 137, 10357−10366

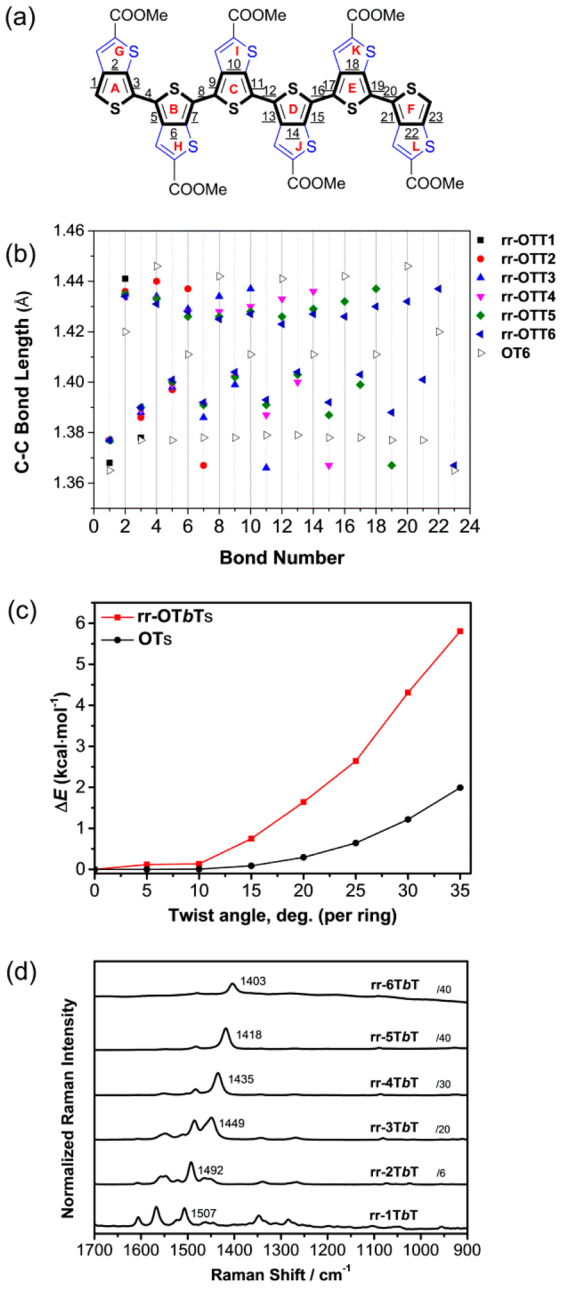

Figure 4. (a) Molecular structure with bond and ring assignments. (b) Bond length alternation pattern in **rr-OT*b*T** derivatives with the **6T** reference. (c) Calculated relative energies required for spiral twisting of **rr-6T*b*T** and **6T** as a function of the twist angle calculated at the B3LYP/TZP level using the ADF program (see part S4 in the Supporting Information). (d) FT-Raman spectra (1064 nm) of **rr-OT*b*T** derivatives in the solid state at room temperature.

Photophysical Properties of Charged rr-6T*b*T. UV−vis-NIR electronic absorption spectra of charged species of these new **OT**s and other carbon-based π-systems recorded in situ can provide valuable information on changes to the π-conjugated backbone when cations and anions are formed. Typically, **OT**s exhibit UV−vis-NIR absorption spectra arising from either oxidized species (aromatic and substituted with electron-donor groups) or reduced species (quinoidal and substituted with electron-acceptor groups), but rarely both.[23] As shown in Figure 5c, oxidation of **rr-6T*b*T** (see the Supporting Information, part S4) produces absorption spectra with a strong band at 1132 nm (weaker features at longer wavelength), whereas the spectra of radical cations (for instance, **6T**) typically generate the strongest bands below 1000 nm (850 nm in $\mathbf{6T}^{+}$),[24] which contrasts here with the much larger red-shifted spectrum for the equivalent [**rr-6T*b*T**]$^{+}$. On the other hand, reduction of **rr-6T*b*T** gives rise to electronic absorption bands at 1013 and 1137 nm because of the radical anion form of **rr-6T*b*T**, [**rr-6T*b*T**]$^{-}$ Figure 5d). Given the inherently electron-rich nature of **OT**s, reports showing the electronic absorption spectra of their anions are very scarce. The similar spectral shapes obtained here for radical anions and cations indicate a similar π-delocalized structure for both injected types of charges, irrespective of the sign. This is another result that reveals the unique conditions for charge conjugation in the **rr-6T*b*T** backbone through either the occupied or empty electroactive frontier orbitals. Unlike **OT**s, **rr-OT*b*T** derivatives are colorful in the neutral state, become colorless to the eye, and are intense NIR-absorbing dyes when they are either oxidized or reduced. These properties, which are valuable for electrochromic materials, are similar to those of poly(ethylenedioxythiophenes), but they now also extend to the cathodic redox branch.[25]

Transient Absorption (TA) Investigations. TA spectroscopy has been used to study the excitation dynamics of the **rr-OT*b*T** compounds in connection with their quinoidal/planar features (see the Supporting Information, part S5). TA spectra for **rr-3T*b*T** are shown in Figure 5 in two different time regimes: (i) after excitation pump with a microsecond flash-photolysis apparatus, which can be used to probe long-lived species, typically triplets, and (ii) with an ultrafast femtosecond pump−probe spectrophotometer (picosecond time regime). From flash-photolysis experiments with excitation at 532 nm in degassed methylcyclohexane, a well-defined TA band in the 600−775 nm range was found (Figure 5a), corresponding to the $T_1 \rightarrow T_n$ absorption from a long-lived triplet species (τ_T = 6 s) formed by ISC.[14] Additionally, from sensitized singlet oxygen measurements from **rr-3T*b*T** (emission at 1270 nm), a singlet oxygen quantum yield of Φ_Δ = 0.35 was obtained, providing an ISC rate constant for **rr-3T*b*T** of 2.7 × 10^9 s^{-1} ($k_{ISC} = \Phi_T (\sim\Phi_\Delta)/\tau_F$). Figure 5b presents the femtosecond TA data with excitation (pump) at 490 nm and probe in the 500−800 nm range for **rr-3T*b*T** in aerated methylcyclohexane. The evolution of the fs-TA spectra with time shows: (i) a TA band centered at approximately 770 nm that arises at early times (Figure 5b) and that decays with time values of 1, 14.7, and 132 ps (see Table S3), which are consistent with those found in the time-correlated single photon counting (TCSPC) fluorescence experiments related to the emission of the relaxed excited state of **rr-3T*b*T**; (ii) at intermediate times, the appearance of a red-shifted TA band with maxima at approximately 925 nm (Figure S12 with the fs-TA spectra collected in the NIR range); and (iii) at longer times, the formation of a TA band that, because of the spectral resemblance with the band obtained with the flash-photolysis setup (Figures 5a), can be attributed to triplet−triplet absorption (see Figure S13). The kinetic data collected in the 600−730 nm range (triplet−triplet absorption) show that this species is formed at the expense of the species present at early times (see Figure 5b inset and Table S3). Furthermore, we have detected that this triplet species is formed with two rising components, 14.68−18.90 ps and 102.2−105.3 ps (Table S3), revealing the existence of two competitive processes during its formation. Similar behavior has been found by investigating the ultrafast dynamics of

DOI: 10.1021/jacs.5b05940
J. Am. Chem. Soc. 2015, 137, 10357−10366

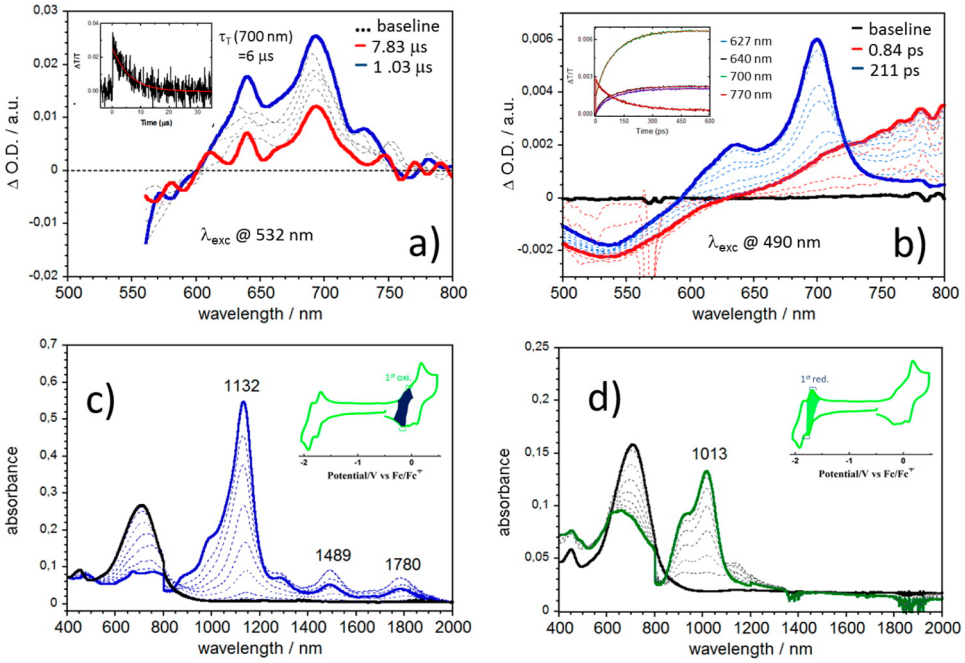

Figure 5. (a) Microsecond and (b) femtosecond TA spectra of **rr-3T*b*T** in methylcyclohexane at room temperature. (c and d) UV−vis-NIR spectroelectrochemistry of **rr-6T*b*T** in 0.1 M Bu_4NPF_6 in CH_2Cl_2 during the first anodic and cathodic one-electron processes, respectively.

terthiophene, **3T**, by wavelength-dependent excitation, and it has been attributed to ultrafast ISC mediated by a twisted nonrelaxed excited-state conformation.[26] Given the almost planar structure of **rr-3T*b*T**, we might rule out this mechanism. In support of this conclusion, when fs-TA spectra were obtained by exciting at the onset of the absorption band of **rr-3T*b*T** (whereby only planar conformers are excited), similar decay/rise time components are found. This result indicates that another ultrafast mechanism is followed for the generation of triplets.

Recently, singlet exciton fission (SEF) has attracted renewed interest in organic electronics because of its potential to overcome the Shockley−Queisser limit of efficiencies of organic photovoltaic cells.[27] In SEF, one singlet excited state splits into two triplets, and the spin-allowed nature of this process means that it can be very efficient. Very recently, we have shown that quinoidal **OT**s fulfill[28] the conditions for SEF, mainly because of the low energy of the T_1 triplet states imparted by planarization/quinoidization. For the investigated quinoidal **rr-3TbT** derivative, TD-DFT B3LYP/TZP quantum chemical calculations predict that the $S_0 \rightarrow S_1$ and $S_0 \rightarrow T_1$ excitations at 2.12 and 1.18 eV, respectively, thus approach the $S_1 \approx 2\ T_1$ (2.18 eV ≈ 2.36 eV) energy requirement for SEF. There is still no consensus concerning a general mechanism for SEF.[29] In fact, another way to observe triplets in short rising times is by the ultrafast formation of geminate radical anions and cations, which could eventually recombine to the neutral triplet species.[30] This process could explain the initial formation of the TA NIR absorption band at approximately 925 nm, which could be ascribed to radical charged species; this assignment is supported by the resemblance of these NIR spectra to those of the radical cations and anions of **rr-6T*b*T** presented in Figure 5c,d, generated in a photoionization process fuelled by their amphoteric redox properties (Figure 2). We therefore propose that, after photoexcitation: (i) the **rr-3T*b*T** singlet excited-state decays rapidly (1 ps) to an intermediate species from which fast triplet generation occurs through SEF with a time constant of 14.68 ps ($k_{SEF} = 6.8 \times 10^{10}\ s^{-1}$); and (ii) charge recombination leads to the neutral rr-**3T*b*T** species assisted by ISC with $k_{ISC} \sim 9.6 \times 10^9\ s^{-1}$ (in the 102.2−105.3 ps range), which is in good agreement with the value obtained from $k_{ISC} = \Phi_T/\tau_F$.

CONCLUSIONS

We have obtained a series of monodisperse oligo(thieno[3,4-*b*]thiophene)s with well-defined and regioregular structures by efficient direct C−H arylation. Strict control of the regioregularity has thus provided an unprecedented series of π-conjugated compounds. The **rr-OT*b*T** derivatives show colors that are tuned in the visible spectrum and amphoteric electrochemical properties due to the small HLGs. These features emerge because of the synergistic effect of the ring fusion on the **T*b*T** unit, which induces a progressive increase in the quinoidization and planarization of the oligomers, giving rise to an exceptionally large effective conjugation length (the largest among the most common π-conjugated hetero-oligomers). In addition, these **T*b*T** oligomers are able to stabilize both cations and anions in a similar manner and behavior. This unique conjugated shape allows a rich photophysics where intersystem crossing, ultrafast triplet (singlet exciton fission), and radical ion generations can coexist. Given these outstanding features, **rr-OT*b*T** derivatives might constitute highly versatile semiconducting materials for use in enhanced optoelectronic devices including ambipolar transistors, electrochromic systems, and photovoltaic cells. After 30 years of research in thiophene-based materials, the **rr-OT*b*T** derivatives developed here might represent one of the newest families of oligothiophenes of this decade.[31]

EXPERIMENTAL SECTION

Materials and General Methods. All the reactions dealing with air- or moisture-sensitive compounds were carried out in a dry reaction vessel under a positive pressure of nitrogen. Unless stated otherwise, starting materials were obtained from Adamas, Aldrich, and J&K and were used without any further purification. Anhydrous THF, toluene,

DOI: 10.1021/jacs.5b05940
J. Am. Chem. Soc. 2015, 137, 10357−10366

and 1,4-dioxane were distilled over Na/benzophenone prior to use. 3,3,3-Triethoxyprop-1-yne,[32] (2,4,6-triisopropylphenyl)boronic acid,[33] and 3-bromo-4-iodothiophene[34] were prepared according to the published procedures. Hydrogen nuclear magnetic resonance (^{1}H NMR) and carbon nuclear magnetic resonance (^{13}C NMR) spectra were measured on Bruker Fourier 300, Bruker Avance 400, and Bruker Avance 600 spectrometers. Chemical shifts for hydrogens are reported in parts per million (ppm, δ scale) downfield from tetramethylsilane and are referenced to the residual protons in the NMR solvent ($CDCl_3$: δ 7.26). ^{13}C NMR spectra were recorded at 75 or 100 MHz. Chemical shifts for carbons are reported in parts per million (ppm, δ scale) downfield from tetramethylsilane and are referenced to the carbon resonance of the solvent ($CDCl_3$: δ 77.2). The data are presented as follows: chemical shift, multiplicity (s = singlet, d = doublet, t = triplet, m = multiplet and/or multiple resonances, br = broad), coupling constant in Hertz (Hz), and integration. EI−MS measurements were performed on UK GCT-Micromass or Shimadzu G-MS-QP2010 spectrometers. MALDI measurements were performed on MALDI-FT 9.4T, Bruker solariX, or MALDI-TOF MS Bruker Autoflex III. Elemental analyses were measured on Flash EA 1112 Series from ThermoQuest. UV−vis and fluorescence spectra were recorded on a Jasco V-570 and Jasco FP-6600 spectrometers, respectively. Cyclic voltammetry (CV) was performed on a CHI620D potentiostat. All measurements were carried out in a one-compartment cell under an N_2 atmosphere, equipped with a glassy-carbon electrode, a platinum counter-electrode, and an Ag/Ag^+ reference electrode with a scan rate of 100 mV/s. The supporting electrolyte was a 0.1 mol/L dichloromethane solution of tetrabutylammonium perchlorate (TBAP). All potentials were corrected against Fc/Fc^+. Fluorescent quantum yields (FLQY) were measured on Absolute PL Quantum Yield Spectrometer C11347 from Hamamatsu. Quantum chemical calculations were performed in the framework of density functional theory as implemented in the Amsterdam Density Functional (ADF) program unless otherwise specified. Simulations were performed in the gas phase. The B3LYP functional and the TZP basis set were used in all calculations. FT-Raman spectra (1064 nm) were obtained by using the FT-Raman accessory kit (FRA/106−S) of a Bruker Equinox 55 FTIR interferometer. A continuous-wave Nd:YAG laser working at 1064 nm was employed for excitation. A germanium detector operating at liquid nitrogen temperature was used. Raman scattering radiation was collected in a backscattering configuration with a standard spectral resolution of 4 cm^{-1}; 1000−3000 scans were averaged for each spectrum. In situ UV−vis-NIR spectroelectrochemical studies were conducted with a Cary 5000 spectrophotometer (Varian) operating in a maximal 175−3300 nm range. A C3 epsilon potentiostat from BASi was used for the electrolysis, with a thin-layer cell from a demountable omni cell (Specac). In this cell, a three-electrode system was coupled to conduct spectroelectrochemistry in situ. A Pt gauze was used as the working electrode, a Pt wire was used as the counter electrode, and a Ag wire was used as the pseudoreference electrode. The spectra were collected at constant potential electrolysis, and the potentials were changed in intervals of 100 mV. The electrochemical medium used was 0.1 M $(C_4H_9)_4NPF_6$ in fresh distilled CH_2Cl_2, at room temperature with sample concentrations of 10^{-3} M. TA spectra were measured with (i) a laser flash-photolysis apparatus pumped by the second harmonic (532 nm) of a Nd:YAG laser (Spectra Physics Quanta-Ray GCR-130); and (ii) HELIOS pump−probe femtosecond TA spectrometer (Ultrafast Systems), equipped with an amplified femtosecond Spectra-Physics Solstice-100F laser.

3-Bromo-4-(3,3,3-triethoxyprop-1-yn-1-yl)thiophene. 3-Bromo-4-iodothiophene **4** (5.78 g, 20.0 mmol), $Pd(PPh_3)_2Cl_2$ (702 mg, 1.0 mmol), CuI (380 mg, 2.0 mmol) were dissolved in degassed triethylamine. 3,3,3-Triethoxyprop-1-yne (4.5 g, 26.0 mmol) was then added and stirred overnight at room temperature. The resulting suspension was filtered and washed with hexane. The combined filtrates were concentrated under reduced pressure and purified on an aluminum-oxide column chromatography (petroleum ether/triethylamine = 20:1) to give 5.7 g of 3-bromo-4-(3,3,3-triethoxyprop-1-yn-1-yl)thiophene in 86% yield as yellowish oil. ^{1}H NMR (300 MHz, $CDCl_3$): δ 1.28 (t, ^3J = 7.2 Hz, 9H), 3.79 (q, ^3J = 7.2 Hz, 6H), 7.25 (d, ^4J = 3.6 Hz, 1H), 7.53 (d, ^4J = 3.6 Hz, 1H); ^{13}C NMR (75 MHz, $CDCl_3$): δ 14.9, 59.1, 86.3, 109.3, 113.5, 122.9, 123.1, 130.5; HRMS (EI) calcd for $C_{13}H_{17}BrO_3S$ $[M]^+$, 332.0082; found, 332.0085.

2-(Triethoxymethyl)thieno[3,4-b]thiophene (1). 3-Bromo-4-(3,3,3-triethoxyprop-1-yn-1-yl)thiophene (5.0 g, 15.1 mmol) in dry diethyl ether (50 mL) was added dropwise *n*-BuLi (9.8 mL, 15.7 mmol, 1.6 M) at −78 °C under N_2 atmosphere and stirred for 1 h. Sulfur powder was then added and stirred for another 1 h. The reaction mixture was warmed to −10 °C over 2 h and then added to a separatory funnel containing ice water (50 mL). The extraction was completed quickly within 1 min. The resulting aqueous layer was slowly heated to 70 °C for 1 h. After cooling to room temperature, the aqueous part was extracted with diethyl ether and dried with $MgSO_4$. The organic layer was evaporated in vacuum, and the residue was purified on an aluminum-oxide column chromatography (petroleum ether/triethylamine = 20:1) to give 2.9 g of compound **3** in 67% yield as a yellow solid. ^{1}H NMR (300 MHz, $CDCl_3$): δ 1.22 (t, ^3J = 7.2 Hz, 9H), 2.53 (q, ^3J = 7.2 Hz, 6H), 7.10 (s, 1H), 7.20 (d, ^4J = 2.7 Hz, 1H), 7.32 (d, ^4J = 2.7 Hz, 1H); ^{13}C NMR (75 MHz, $CDCl_3$): δ 15.0, 58.2, 110.7, 112.6, 112.8, 117.1, 139.2, 146.5, 148.9; HRMS (EI) calcd for $C_{13}H_{18}O_3S_2$ $[M]^+$, 286.0697; found, 286.0702.

*Ethyl 6-Iodothieno[3,4-b]thiophene-2-carboxylate (**2a**) and Ethyl 4-Iodothieno[3,4-b]thiophene-2-carboxylate (**2b**).* To a solution of 2-(triethoxymethyl)thieno[3,4-*b*]thiophene **1** (5.72 g, 20.0 mmol) in dry THF was dropped *n*-BuLi/*n*-hexane (12.5 mL, 20.0 mmol, 1.6 M) at −78 °C and stirred for 1 h. 1,2-Diiodoethane (5.64 g, 20.0 mmol) was then added and stirred for another 1 h. After warming to room temperature, the reaction solution was added HCl (1.0 M), extracted with CH_2Cl_2, and purified by an aluminum-oxide column chromatography (petroleum ether/triethylamine = 20:1) to give 4.07 and 1.35 g of compounds **2a** (60%) and **2b** (20%) as purple and brown solids, respectively. **2a**: ^{1}H NMR (300 MHz, $CDCl_3$): δ 1.39 (t, ^3J = 7.2 Hz, 3H); 4.38 (q, ^3J = 7.2 Hz, 2H), 7.66 (s, 1H), 7.80 (s, 1H); ^{13}C NMR (100 MHz, $CDCl_3$): δ 14.3, 57.6, 61.8, 123.1, 124.3, 140.1, 145.4, 147.8, 162.8; HRMS (EI) calcd for $C_9H_7IO_2S_2$ $[M]^+$: 337.8932, found, 337.8928. **2b**: ^{1}H NMR (300 MHz, $CDCl_3$): δ 7.50 (s, 1H), 7.42 (s, 1H), 4.38 (q, ^3J = 7.2 Hz, 2H), 1.40 (t, ^3J = 7.2 Hz, 3H); ^{13}C NMR (100 MHz, $CDCl_3$): δ 14.3, 57.6, 61.8, 123.1, 124.3, 140.1, 145.4, 147.8, 162.8; HRMS (EI) calcd for $C_9H_7IO_2S_2$ $[M]^+$, 337.8932; found, 337.8935.

Octyl 6-Iodothieno[3,4-b]thiophene-2-carboxylate. To a solution of compound **2a** (3.40 g, 10.0 mmol) in ethanol (50 mL) was added LiOH (0.72 g, 30.0 mmol) and then heated to 78 °C for 2 h under inert atmosphere. After cooling to room temperature, HCl (40 mL, 1.0 M) was added and stirred for another 30 min. The resulting suspension was extracted with ethyl acetate and dried over $MgSO_4$. The solvent was evaporated in vacuum to give 2.95 g of 6-iodothieno[3,4-*b*]thiophene-2-carboxylic acid in 95% yield as a solid which was directly used in the next step without further purification. (^{1}H NMR (300 MHz, d^6-DMSO): δ 7.84 (s, 1H), 8.01 (s, 1H); ^{13}C NMR (100 MHz, d^6-DMSO): δ 61.8, 124.7, 125.1, 140.4, 145.2, 146.2, 163.6; ESI-MS: 310 $[M]^+$.) 6-Iodothieno[3,4-*b*]thiophene-2-carboxylic acid (3.1 g, 10.0 mmol), dicyclohexylcarbodiimide (2.5 g, 12.0 mmol), 4-dimethylaminopyridine (430 mg, 3.5 mmol) were dissolved in dry CH_2Cl_2 (100 mL) with a round-bottom flask. 1-Octanol (7.9 mL, 50.0 mmol) was added to the reaction mixture at room temperature and stirred for 24 h under inert atmosphere. The resulting mixture was poured into water and extracted with dichloromethane. The organic layer was concentrated under reduced pressure and purified on a silica-gel column chromatography (petroleum ether/CH_2Cl_2 = 4:1) to give 3.2 g of compound **3a** in 74% yield as dark-red oil. ^{1}H NMR (300 MHz, $CDCl_3$): δ 0.88 (t, ^3J = 6.9, 3H), 1.29−1.42 (m, 10H), 1.78 (q, ^3J = 6.9, 2H), 4.30 (t, ^3J = 6.9, 2H), 7.65 (s, 1H), 7.79 (s, 1H); ^{13}C NMR (75 MHz, $CDCl_3$) δ 14.32, 22.86, 26.13, 28.81, 29.38, 29.40, 31.99, 57.80, 66.15, 123.27, 124.48, 140.31, 145.55, 147.96,163.05; HRMS (EI) calcd for $C_{15}H_{19}IO_2S_2$ $[M]^+$, 421.9871; found, 421.9869.

*Octyl 4-Iodothieno[3,4-b]thiophene-2-carboxylate (**3b**).* Dark-brown oil (73%). ^{1}H NMR (300 MHz, $CDCl_3$): δ 0.88 (t, ^3J = 6.9, 3H), 1.29−1.42 (m, 10H), 1.76 (q, ^3J = 6.9, 2H), 4.31 (t, ^3J = 6.9, 2H),

DOI: 10.1021/jacs.5b05940
J. Am. Chem. Soc. 2015, 137, 10357−10366

7.42 (s, 1H), 7.49 (s, 1H); ^{13}C NMR (75 MHz, $CDCl_3$): δ 14.3, 22.9, 26.1, 28.8, 29.39, 29.42, 32.0, 66.2, 118.1, 124.2, 138.9, 141.1, 151.4, 163.1; EI-MS: 422 $[M]^+$.

Octyl 6-(Tributylstannyl)thieno[3,4-b]thiophene-2-carboxylate. To a solution of octyl 6-iodothieno[3,4-*b*]thiophene-2-carboxylate (844 mg, 2.0 mmol) in dry THF (10 mL) was dropped *i*-PrMgCl/THF (1.1 mL, 2.2 mmol, 2.0 M) at −40 °C and stirred for 1 h. Tri-*n*-butyltin chloride (0.55 mL, 2.2 mmol) was then added and stirred for another 1 h. The reaction was quenched with saturated aqueous NH_4Cl and extracted with CH_2Cl_2. After dried over sodium sulfate, the solvent was evaporated in vacuum to give brown oil. ^{1}H NMR (300 MHz, $CDCl_3$): δ 0.88 (m, 12H), 1.29−1.42 (m, 22H), 1.67 (m, 6H), 1.76 (m, 2H), 4.31 (t, ^3J = 6.9, 2H), 7.86 (s, 1H), 7.74 (s, 1H); EI-MS: 586 $[M]^+$.

Octyl 4-(Tributylstannyl)thieno[3,4-b]thiophene-2-carboxylate. ^{1}H NMR (300 MHz, $CDCl_3$): δ 0.88 (m, 12H), 1.29−1.42 (m, 22H), 1.67 (m, 6H), 1.76 (m, 2H), 4.32 (t, ^3J = 6.9, 2H), 7.42 (s, 1H), 7.49 (s, 1H); EI-MS: 586 $[M]^+$.

*Octyl 6-(2,4,6-Triisopropylphenyl)thieno[3,4-b]thiophene-2-carboxylate (**B$_1$**-H).* Octyl 6-iodothieno[3,4-*b*]thiophene-2-carboxylate **3a** (844 mg, 2.0 mmol), $Pd(PPh_3)_2Cl_2$ (140 mg, 0.2 mmol), Cs_2CO_3 (1.96 g, 6.0 mmol) were added degassed dioxane (8 mL), to which (2,4,6-triisopropylphenyl)boronic acid (744 mg, 3.0 mmol) was added and stirred at 80 °C for 24 h. The resulting suspension was filtered and washed with dichloromethante. The combined filtrates were concentrated under reduced pressure and purified on a silica-gel column chromatography to give 926 mg of pure compound **B$_1$**-H in 93% yield as orange oil. ^{1}H NMR (300 MHz, $CDCl_3$): δ 0.88 (t, ^3J = 6.6, 3H), 1.13 (d, ^3J = 6.9, 6H), 1.15 (d, ^3J = 6.9, 6H), 1.28−1.42 (m, 18H), 1.73 (q, ^3J = 6.9, 2H), 2.70 (m, 2H), 2.96 (m, 1H), 4.29 (t, ^3J = 6.6, 2H), 7.09 (s, 2H), 7.64 (s, 1H), 7.71 (s, 1H); ^{13}C NMR (75 MHz, $CDCl_3$): δ 14.1, 22.6, 24.0, 24.7, 24.7, 25.9, 28.6, 29.17, 29.20, 31.8, 34.4,30.9, 65.7, 116.4, 121.1, 124.0, 125.5, 127.7, 139.4, 139.9, 145.1, 149.6, 150.2, 163.3; HRMS (MALDI-TOF) calcd for $C_{30}H_{42}O_2S_2$ $[M]^+$, 498.2626; found, 498.2630.

*Octyl 4-(2,4,6-Triisopropylphenyl)thieno[3,4-b]thiophene-2-carboxylate (**A$_1$**-H).* Orange oil (89%). ^{1}H NMR (300 MHz, $CDCl_3$): δ 0.88 (t, ^3J = 6.6, 3H), 1.06 (d, ^3J = 6.9, 6H), 1.22 (d, ^3J = 6.9, 6H), 1.26−1.42 (m, 18H), 1.71 (q, ^3J = 6.9, 2H), 2.63 (m, 2H), 2.96 (m, 1H), 4.25 (t, ^3J = 6.6, 2H), 7.08 (s, 2H), 7.29 (s, 1H), 7.34 (s, 1H); ^{13}C NMR (100 MHz, $CDCl_3$): δ 14.1, 22.6, 24.0, 24.5, 24.6, 25.9, 28.6, 29.2, 30.8, 31.7, 34.4, 65.7, 110.6, 120.9, 123.3, 125.8, 133.9, 138.8, 139.3, 145.3, 149.5, 150.1, 163.2; HRMS (MALDI-TOF) calcd for $C_{30}H_{42}O_2S_2$ $[M]^+$, 498.2626; found, 498.2628.

*Octyl 4-Bromo-6-(2,4,6-triisopropylphenyl)thieno[3,4-b]thiophene-2-carboxylate (**B$_1$**-Br).* To a solution of **B$_1$-H** (847 mg, 1.7 mmol) in chloroform was added *N*-bromosuccinimide (363 mg, 2.0 mmol) in the dark and stirred for 12 h at room temperature. The reaction mixture was added water, saturated aqueous $NaHSO_3$ and $NaHCO_3$ successively, extracted with dichloromethane, and purified on a silica-gel column chromatography to give 883 mg of compound **B$_1$**-Br in 90% yield as orange oil. ^{1}H NMR (400 MHz, $CDCl_3$): δ 0.87 (t, ^3J = 6.8, 3H), 1.13 (d, ^3J = 6.8, 6H), 1.15 (d, ^3J = 6.8, 6H), 1.28−1.42 (m, 18H), 1.72 (q, ^3J = 7.2, 2H), 2.74 (m, 2H), 2.94 (m, 1H), 4.28 (t, ^3J = 6.8, 2H), 7.07 (s, 2H), 7.57 (s, 1H); ^{13}C NMR (100 MHz, $CDCl_3$): δ 14.1, 22.6, 24.0, 24.7, 24.8, 25.9, 28.6, 29.16, 29.19, 31.0, 31.8, 34.4, 66.0, 101.7, 121.1, 121.2, 123.0, 124.7, 129.1, 138.4, 140.7, 145.4, 149.7, 150.7, 162.9; HRMS (MALDI-TOF) calcd for $C_{30}H_{41}BrO_2S_2$ $[M]^+$, 576.1731; found, 576.1733.

*Octyl 6-Bromo-4-(2,4,6-triisopropylphenyl)thieno[3,4-b]thiophene-2-carboxylate (**A$_1$**-Br).* Orange oil (83%). ^{1}H NMR (400 MHz, $CDCl_3$): δ 0.87 (t, ^3J = 6.8, 3H), 1.13 (d, ^3J = 6.8, 6H), 1.15 (d, ^3J = 6.8, 6H), 1.28−1.42 (m, 18H), 1.71 (q, ^3J = 7.2, 2H), 2.70 (m, 2H), 2.95 (m, 1H), 4.26 (t, ^3J = 6.8, 2H), 7.08 (s, 2H), 7.32 (s, 1H); ^{13}C NMR (100 MHz, $CDCl_3$): δ 14.1, 22.6, 24.0, 24.56, 24.57, 25.9, 28.6, 29.2, 30.8, 31.8, 34.4, 65.9, 96.4, 121.1, 123.9, 124.9, 135.6, 139.8, 140.3, 144.8, 149.6, 150.6, 162.8; HRMS (MALDI-TOF) calcd for $C_{30}H_{41}BrO_2S_2$ $[M]^+$, 576.1731; found, 576.1730.

*Dioctyl 6-(2,4,6-Triisopropylphenyl)-[4,6′-bithieno[3,4-b]thiophene]-2,2′-dicarboxylate (**B$_2$**-H).* **B$_1$**-Br (865 mg, 1.5 mmol), $Pd(PPh_3)_4$ (87 mg, 0.075 mmol), and octyl 6-(tributylstannyl)thieno-[3,4-*b*]thiophene-2-carboxylate (970 mg, 1.65 mmol) were dissolved in degassed toluene (6 mL) and stirred at 100 °C for 36 h. The reaction mixture was filtered and washed with dichloromethane. The combined filtrates were concentrated under reduced pressure and purified on a silica-gel column chromatograph to give 594 mg of compound **B$_2$**-H in 50% yield as an orange solid. ^{1}H NMR (400 MHz, $CDCl_3$): δ 0.88 (m, 6H), 1.27−1.42 (m, 40H), 1.71−1.84 (m, 4H), 2.80 (m, 2H), 2.96 (m, 1H), 4.29−4.35 (m, 4H), 7.10 (s, 2H), 7.63 (s, 1H), 7.72 (s, 1H), 8.10 (s, 1H); ^{13}C NMR (100 MHz, $CDCl_3$): δ 13.8, 14.3, 22.8, 24.2, 24.9, 25.0, 26.1, 27.0, 28.8, 29.37, 29.40 31.3, 32.0, 34.7, 66.1, 66.2, 116.2, 121.5, 123.2, 124.1, 124.4, 124.9, 126.9, 127.6, 136.1, 140.4, 140.8, 146.3, 149.9, 150.8, 163.1, 163.3; HRMS (MALDI-TOF) calcd for $C_{45}H_{60}O_4S_4$ $[M]^+$, 792.3374; found, 792.3370.

*4′-(2,4,6-Triisopropylphenyl)-[4,6′-bithieno[3,4-b]thiophene]-2,2′-dicarboxylate (**A$_2$**-H).* Orange solid (58%). ^{1}H NMR (400 MHz, $CDCl_3$): δ 0.95 (m, 6H), 1.10−1.42 (m, 40H), 1.78−1.73 (m, 4H), 2.77 (m, 2H), 2.96 (m, 1H), 4.28−4.33 (m, 4H), 7.12 (s, 2H), 7.30 (s, 1H), 7.39 (s, 1H), 8.02 (s, 1H); ^{13}C NMR (100 MHz, $CDCl_3$): δ 14.1, 22.6, 22.7, 24.0, 24.6, 24.7, 25.9, 28.6, 28.7, 29.17, 29.19, 31.0, 31.8, 34.5, 65.9, 66.0, 109.6, 121.1, 122.1, 123.6, 123.7, 124.9, 127.8, 134.2, 135.3, 139.9, 140.1, 140.7, 140.9, 145.7, 149.6, 150.6, 162.8, 162.9; HRMS (MALDI-TOF) calcd for $C_{45}H_{60}O_4S_4$ $[M]^+$, 792.3374; found, 792.3369.

*Dioctyl 4′-Bromo-6-(2,4,6-triisopropylphenyl)-[4,6′-bithieno[3,4-b]thiophene]-2,2′-dicarboxylate (**B$_2$**-Br).* To a solution of **B$_2$**-H (158 mg, 0.2 mmol) in $CHCl_3$/DMF (6:1) was added *N*-bromosuccinimide (43 mg, 0.24 mmol) in the dark. The reaction mixture was stirred for 2 h at room temperature and added water, saturated aqueous $NaHSO_3$ and $NaHCO_3$ successively. The reaction suspension was extracted with dichloromethane and purified on a silica-gel column chromatography to give 52 mg of compound **B$_2$**-Br in 30% yield as an orange solid. ^{1}H NMR (400 MHz, $CHCl_3$): δ 0.88 (m, 6H), 1.27−1.42 (m, 40H), 1.72−1.80 (m, 4H), 2.80 (m, 2H), 2.97 (m, 1H), 4.34−4.30 (m, 4H), 7.11 (s, 2H), 7.60 (s, 1H), 8.00 (s, 1H); ^{13}C NMR (100 MHz, $CDCl_3$): δ 14.3, 22.8, 24.2, 24.9, 25.0, 26.1, 28.8, 29.3, 29.4, 31.3, 31.9, 34.7, 66.2, 66.4, 121.5, 123.1, 123.9, 124.3, 124.7, 126.6, 127.5, 134.7, 140.5, 140.92, 140.94, 141.5, 146.5, 150.0, 150.9, 162.7, 163.1; HRMS (MALDI-TOF) calcd for $C_{45}H_{59}BrO_4S_4$ $[M]^+$, 870.2480; found, 870.2483.

*6-Bromo-4′-(2,4,6-triisopropylphenyl)-[4,6′-bithieno[3,4-b]thiophene]-2,2′-dicarboxylate (**A$_2$**-Br).* Orange solid (82%). ^{1}H NMR (400 MHz, $CDCl_3$): δ 0.88 (m, 6H), 1.17−1.41 (m, 40H), 1.72−1.77 (m, 4H), 2.74 (m, 2H), 2.97 (m, 1H), 4.29−4.31 (m, 4H), 7.11 (s, 2H), 7.38 (s, 1H), 7.98 (s, 1H); ^{13}C NMR (100 MHz, $CDCl_3$): δ 14.3, 22.8, 24.2, 24.8, 24.9, 26.1, 28.8, 29.36, 29.38, 31.2, 32.0, 34.7, 66.3, 121.4, 121.5, 123.8, 124.6, 135.1, 136.0, 139.8, 140.3, 140.4, 142.6, 146.0, 149.7, 150.9, 162.7, 162.8; HRMS (MALDI-TOF) calcd for $C_{45}H_{59}BrO_4S_4$ $[M]^+$, 870.2480; found, 870.2478.

*6-(2,4,6-Triisopropylphenyl)-[4,6′:4′,6″-terthieno[3,4-b]thiophene]-2,2′,2″-tricarboxylate (**B$_3$**-H).* **B$_2$-Br** (130 mg, 0.15 mmol), $Pd(PPh_3)_4$ (8.7 mg, 0.0075 mmol), and octyl 6-(tributylstannyl)thieno[3,4-*b*]thiophene-2-carboxylate (97 mg, 0.165 mmol) were dissolved in degassed toluene (3 mL) and stirred at 100 °C for 36 h. The resulting suspension was filtered and washed with dichloromethane. The combined filtrates were concentrated under reduced pressure and purified on a silica-gel column chromatograph to give 73 mg of compound **B$_3$**-H in 45% yield as a purple-red solid. ^{1}H NMR (400 MHz, $CDCl_3$): δ 1.17 (m, 9H), 1.27−1.45 (m, 50H), 1.73−1.82 (m, 6H), 2.83 (m, 2H), 2.97 (m, 1H), 4.31−4.38 (m, 6H), 7.11 (s, 2H), 7.67 (s, 1H), 7.74 (s, 1H), 8.10 (s, 1H), 8.13 (s, 1H); ^{13}C NMR (100 MHz, $CDCl_3$): δ 14.3, 22.8, 24.9, 24.2, 25.0, 26.1, 28.8, 28.9, 29.4, 31.4, 31.99, 32.03 34.7, 66.1, 66.30, 66.34, 117.3, 121.5, 121.7, 122.5, 124.0, 124.3, 124.4, 124.9, 127.0, 127.6, 137.2, 137.3, 140.5, 140.6, 140.8, 141.0, 141.1, 141.5, 146.6, 150.0, 150.9, 162.8, 162.9, 163.2; HRMS (MALDI-TOF) calcd for $C_{60}H_{78}O_6S_6$ $[M]^+$, 1086.4123; found, 1086.4111.

*Trioctyl 6-Chloro-4″-(2,4,6-triisopropylphenyl)-[4,6′:4′,6″-terthieno[3,4-b]thiophene]-2,2′,2″-tricarboxylate (**A$_3$**-Cl).* **A$_2$**-Br (87

DOI: 10.1021/jacs.5b05940
J. Am. Chem. Soc. 2015, 137, 10357−10366

mg, 0.1 mmol), $Pd(PPh_3)_4$ (6 mg, 0.005 mmol), and octyl 6-chloro-4-(tributylstannyl)thieno[3,4-*b*]thiophene-2-carboxylate (68 mg, 0.11 mmol) were dissolved in degassed toluene (2 mL) and stirred at 100 °C for 24 h. The resulting suspension was filtered and washed with dichloromethane. The combined filtrates were concentrated under reduced pressure and purified on a silica-gel column chromatograph to give 33 mg of compound **A**$_3$-Cl in 30% yield as a purple solid. ^{1}H NMR (400 MHz, $CDCl_3$): δ 0.88 (m, 9H), 1.17−1.41 (m, 48H), 1.73−1.84 (m, 6H), 2.77 (m, 2H), 2.98 (m, 1H), 4.30−4.37 (m, 4H), 7.13 (s, 2H), 7.41 (s, 1H), 8.04 (s, 1H), 8.05 (s, 1H); ^{13}C NMR (100 MHz, $CDCl_3$): δ 14.3, 22.8, 24.2, 24.8, 24.9, 26.11, 26.15 26.2, 28.8, 29.36, 29.39, 31.3, 31.97, 32.02, 34.7, 66.29, 66.33, 66.4, 115.3, 119.8, 121.4, 121.6, 123.8, 124.4, 124.5, 124.9, 125.7, 128.2, 136.0, 136.5, 138.1, 139.2, 139.9, 140.5, 140.8, 140.7, 141.0, 146.3, 149.7, 151.0, 162.7, 162.8; HRMS (MALDI-TOF) calcd for $C_{60}H_{77}ClO_6S_6$ $[M]^+$, 1120.3733; found, 1120.3730.

Tetraoctyl 4‴-(2,4,6-triisopropylphenyl)-[4,6′:4′,6″:4″,6‴-quaterthieno[3,4-*b*]thiophene]-2,2′,2″,2‴-tetracarboxylate (***A*$_4$*-H***). **A**$_3$-Cl (22 mg, 0.02 mmol), $Pd(t\text{-}Bu_3P)_2Cl_2$ (2 mg, 0.004 mmol), and octyl 4-(tributylstannyl)thieno[3,4-*b*]thiophene-2-carboxylate were dissolved in degassed toluene (2 mL) and stirred at 100 °C for 24 h. The resulting suspension was filtered and washed with CH_2Cl_2. The combined filtrates were concentrated under reduced pressure and purified on a silica-gel column chromatograph to give 14 mg of compound **A**$_4$-H in 50% yield as a dark-blue solid. ^{1}H NMR (400 MHz, $CDCl_3$): δ 0.83−0.88 (m, 12H), 1.20−1.36 (m, 60H), 1.76−1.86 (m, 8H), 2.79 (m, 2H), 2.99 (m, 1H), 4.30−4.42 (m, 8H), 7.15 (s, 1H), 7.32 (s, 1H), 7.43 (s, 1H), 8.07 (s, 1H), 8.11 (s, 1H), 8.17 (s, 1H); ^{13}C NMR (125 MHz, $CDCl_3$): δ 14.1, 22.6, 24.0, 24.6, 24.7, 25.88, 25.91, 25.98, 26.00, 28.7, 29.2, 29.3, 29.7, 31.1, 31.81, 31.83, 31.8, 34.5, 65.9, 66.12, 66.16, 66.2, 110.4, 120.1, 121.2, 121.7, 123.5, 124.06, 124.11, 124.7, 126.6, 126.9, 128.1, 140.2, 140.50, 140.54, 140.6, 140.8, 140.9, 141.2, 146.1, 149.5, 150.8, 162.4, 162.5, 162.6, 162.7; HRMS (MALDI-TOF) calcd for $C_{60}H_{82}O_4S_4$ $[M]^+$, 1380.4871; found, 1380.4867.

*Ethyl 4,6-bis(2,4,6-triisopropylphenyl)thieno[3,4-b]thiophene-2-carboxylate (**rr-1TbT**).* Ethyl 4,6-dibromothieno[3,4-*b*]thiophene-2-carboxylate (74 mg, 0.2 mmol), $Pd(PPh_3)_2Cl_2$ (28 mg, 0.04 mmol), (2,4,6-triisopropylphenyl)boronic acid (198 mg, 0.8 mmol), and Cs_2CO_3 (391 mg, 1.2 mmol) were dissolved in degassed dioxane (3 mL) and stirred at 80 °C for 24 h. The resulting suspension was filtered and washed with dichlormethane. The combined filtrates were concentrated under reduced pressure and purified on a silica-gel column chromatography (petroleum ether/CH_2Cl_2 = 10:1) to give 70 mg of compound

rr-1TbT. White solid (57%). ^{1}H NMR (400 MHz, $CDCl_3$): δ 1.14−1.34 (m, 39H), 2.77−2.89 (m, 4H), 2.91−3.02 (m, 2H), 4.30 (q, ^3J = 7.2 Hz, 2H), 7.10 (s, 2H), 7.11 (s, 2H), 7.39 (s, 1H); ^{13}C NMR (100 MHz, $CDCl_3$) δ 14.3, 24.0, 24.2, 24.4, 24.75, 24.78, 31.0, 31.1, 34.4, 61.4, 120.9, 121.1, 123.9, 125.7, 126.0, 126.8, 133.7, 137.9, 139.2, 144.3, 149.3, 149.4, 149.96, 150.02, 163.3; HRMS (MALDI-TOF) calcd for $C_{39}H_{52}O_2S_2$ $[M]^+$, 616.3409; found, 616.3402.

*Dioctyl 4′,6-bis(2,4,6-triisopropylphenyl)-[4,6′-bithieno[3,4-b]-thiophene]-2,2′-dicarboxylate (**rr-2TbT**).* Orange solid (86%). ^{1}H NMR (300 MHz, $CDCl_3$): δ 0.83−0.87 (m, 6H), 1.17−1.35 (m, 56H), 1.69−1.78 (m,4H), 2.75−2.89 (m, 4H), 2.93−3.03 (m, 2H), 4.26−4.31 (m, 4H), 7.12 (s, 2H), 7.13 (s, 2H), 7.40 (s, 1H), 8.06 (s, 1H); ^{13}C NMR (100 MHz, $CDCl_3$): δ 14.1, 22.6, 24.0, 24.6, 24.68, 24.70, 24.8, 25.9, 28.6, 29.1, 29.2, 31.0, 31.2, 31.7, 34.5, 65.9, 66.0, 121.1, 121.2, 122.4, 123.6, 124.3, 124.9, 125.0, 126.2, 127.7, 133.8, 134.9, 139.7, 139.9, 140.2, 140.6, 145.7, 149.6, 149.8, 150.58, 150.62, 162.8, 163.1; HRMS (MALDI-TOF) calcd for $C_{60}H_{82}O_4S_4$ $[M]^+$, 994.5096; found, 994.5098.

Hexaoctyl 4′‴′,6-bis(2,4,6-triisopropylphenyl)-[4,6′:4′,6″:4″,6‴:4‴,6‴′,4‴′,6′‴′-sexithieno[3,4-*b*]thiophene]-2,2′,2″,2‴,2‴′,2‴′-hexacarboxylate (***rr-6TbT***). **A**$_4$-H (23 mg, 0.017 mmol), **B**$_2$-Br (18 mg, 0.02 mmol), $Pd(OAc)_2$ (1 mg, 0.004 mmol), PPh_3 (2 mg, 0.008 mmol), and Cs_2CO_3 (11 mg, 0.034 mmol) were dissolved in degassed toluene (2 mL) in the dark, and the mixture was stirred at 80 °C for 36 h. The resulting suspension was filtered and washed with dichloromethane. The combined filtrates were concentrated under reduced pressure and purified by silica-gel column chromatography (petroleum ether/CH_2Cl_2 = 1:1) to give **rr-6T*b*T** (23 mg, 62%) as a black solid. ^{1}H NMR (400 MHz, $CDCl_3$): δ 0.83−0.87 (m, 18H), 1.12−1.45 (m, 96H), 1.75−1.90 (m, 12H), 2.76−2.88 (m, 4H), 2.94−3.03 (m, 2H), 4.32−4.45 (m, 12H), 7.12 (s, 2H), 7.15 (s, 2H), 7.43 (s, 1H), 8.11 (s, 1H), 8.18 (s, 1H), 8.21 (s, 1H), 8.24 (s, 1H), 8.25 (s, 1H); ^{13}C NMR (125 MHz, $CDCl_3$): δ 14.1, 22.6, 24.0, 24.6, 24.7, 24.8, 25.9, 26.0, 28.66, 28.71, 29.2, 29.7, 29.8, 31.1, 31.2, 31.8, 31.9, 34.5, 65.9, 66.1, 66.2, 119.9, 121.0, 121.2, 121.3, 124.2, 124.6, 124.7, 126.8, 138.5, 138.8, 140.6, 140.7, 140.89, 140.95, 141.0, 141.3, 149.5, 149.8, 162.4, 162.5, 162.6, 162.9; HRMS (MALDI-TOF, *m*/*z*): calcd for $C_{75}H_{100}O_6S_6$, 2170.8089; found, 2170.8099.

*Trioctyl 4″,6-bis(2,4,6-triisopropylphenyl)-[4,6′:4′,6″-terthieno-[3,4-b]thiophene]-2,2′,2″-tricarboxylate (**rr-3TbT**).* Purple-red solid (49%). ^{1}H NMR (400 MHz, $CDCl_3$): δ 0.83−0.87 (m, 9H), 1.17−1.43 (m, 66H), 1.69−1.77 (m, 6H), 2.78−2.86 (m, 4H), 2.96−3.00 (m, 2H), 4.30−4.35 (m, 6H), 7.12 (s, 2H), 7.14 (s, 2H), 7.42 (s, 1H), 8.07 (s, 1H), 8.17 (s, 1H); ^{13}C NMR (100 MHz, $CDCl_3$): δ 14.5, 22.60, 22.63, 24.0, 24.6, 24.69, 24.74, 24.8, 25.88, 25.90, 25.95, 28.6, 29.1, 29.2, 31.0, 31.1, 31.7, 31.8, 34.5, 65.9, 66.0, 66.1, 121.0, 121.2, 121.3, 121.7, 123.6, 124.2, 124.7, 124.8, 127.0, 127.2, 135.2, 136.0, 137.2, 140.25, 140.30, 140.32, 140.4, 140.9, 146.1, 149.6, 149.8, 150.6, 150.7, 162.6, 162.7, 163.0; HRMS (MALDI-TOF) calcd for $C_{75}H_{100}O_6S_6$ $[M]^+$, 1288.5844; found, 1288.5833.

Tetraoctyl 4‴,6-bis(2,4,6-triisopropylphenyl)-[4,6′:4′,6″:4″,6‴-quaterthieno[3,4-*b*]thiophene]-2,2′,2″,2‴-tetracarboxylate (***rr-4TbT***). Dark-blue solid (60%). ^{1}H NMR (400 MHz, $CDCl_3$): δ 0.83−0.87 (m, 12H), 8.20 (s, 1H), 1.17−1.45 (m, 76H), 1.74−1.84 (m, 8H), 2.76−2.88 (m, 4H), 2.94−3.03 (m, 2H), 4.31−4.39 (m, 8H), 7.12 (s, 2H), 7.14 (s, 2H), 7.43 (s, 1H), 8.10 (s, 1H), 8.17 (s, 1H); ^{13}C NMR (100 MHz, $CDCl_3$): δ 14.3, 22.8, 24.2, 24.8, 24.9, 24.96, 25.02, 26.08, 26.11, 26.2, 28.9, 29.4, 31.2, 31.4, 32.0, 34.7, 66.1, 66.30, 66.34, 66.4, 120.4, 121.4, 121.5, 121.8, 121.9, 123.8, 124.4, 124.5, 124.9, 126.4, 127.0, 127.7, 128.3, 135.9, 136.6, 137.6, 138.5, 140.56, 140.64, 140.7, 140.9, 141.17, 141.24, 141.5, 146.3, 149.8, 150.0, 150.9, 151.0, 162.7, 162.8, 162.9, 163.2; HRMS (MALDI-TOF) calcd for $C_{75}H_{100}O_6S_6$ $[M]^+$, 1582.6592; found, 1582.6580.

Pentaoctyl 4‴′,6-bis(2,4,6-triisopropylphenyl)-[4,6′:4′,6″:4″,6‴:4‴,6‴′-quinquethieno[3,4-*b*]thiophene]-2,2′,2″,2‴,2‴′-pentacarboxylate (***rr-5TbT***). Black solid (48%). ^{1}H NMR (400 MHz, $CDCl_3$): δ 0.83−0.88 (m, 15H), 1.12−1.45 (m, 86H), 1.76−1.83 (m, 10H), 2.76−2.88 (m, 4H), 2.94−3.03 (m, 2H), 4.32−4.43 (m, 10H), 7.13 (s, 2H), 7.15 (s, 2H), 7.44 (s, 1H), 8.11 (s, 1H), 8.18 (s, 1H), 8.21 (s, 1H), 8.24 (s, 1H); ^{13}C NMR (125 MHz, $CDCl_3$): δ 14.1, 22.6, 24.0, 24.6, 24.67, 24.75, 24.8, 25.9, 26.0, 28.7, 29.2, 29.3, 29.7, 31.1, 31.2, 31.79, 31.84, 34.5, 65.9, 66.11, 66.14, 66.2, 120.0, 121.2, 121.3, 121.5, 123.6, 124.3, 124.7, 126.0, 126.8, 127.3, 136.5, 138.5, 138.6, 140.4, 140.5, 140.6, 140.76, 140.82, 141.0, 141.2, 146.2, 149.5, 149.8, 150.7, 150.9, 162.46, 162.55, 162.6, 162.9; HRMS (MALDI-TOF) calcd for $C_{75}H_{100}O_6S_6$ $[M]^+$, 1876.7341; found, 1876.7339.

■ ASSOCIATED CONTENT

Supporting Information

Synthesis of **PT*b*T**, NMR spectra, theoretical calculation details, cif files of **rr-2T*b*T** without terminal 2,4,6-triisopropylphenyl groups, and details of photophysics. The Supporting Information is available free of charge on the ACS Publications website at DOI: 10.1021/jacs.5b05940.

■ AUTHOR INFORMATION

Corresponding Authors

*xzzhu@iccas.ac.cn

*casado@uma.es

Notes

The authors declare no competing financial interest.

DOI: 10.1021/jacs.5b05940
J. Am. Chem. Soc. 2015, 137, 10357−10366

■ ACKNOWLEDGMENTS

We thank the National Basic Research Program of China (973 Program) (no. 2014CB643502), the Strategic Priority Research Program of the Chinese Academy of Sciences (XDB12010200), and the National Natural Science Foundation of China (91333113) for financial support. The Coimbra Chemistry Centre thank FCT (project PEst-OE/QUI/UI0313/2014 and Program C2008-DRH05-11-842) for financial support. The research leading to these results has received funding from Laserlab-Europe (grant agreement no. 284464, EC's Seventh Framework Programme). M.M.O. acknowledges financial support from the Marie Curie COFUND programme "U-Mobility" cofinanced by Universidad de Malaga and the European Community's Seventh Framework Programme under grant agreement no. 246550. The work at the University of Málaga was supported by MINECO through project reference CTQ2012-33733 and by the Junta de Andalucía through research project P09-FQM-4708.

■ REFERENCES

(1) *Semiconducting and Metallic Polymers*; Heeger, A. J., Sariciftci, N. S., Namdas, E. B., Eds.; Oxford University Press Inc.: New York, 2010.
(2) Wudl, F.; Kobayashi, M.; Heeger, A. J. *J. Org. Chem.* **1984**, *49*, 3382.
(3) Kertesz, M.; Choi, C. H.; Yang, S. *Chem. Rev.* **2005**, *105*, 3448.
(4) (a) Chen, H.-Y.; Hou, J.; Zhang, S.; Liang, Y.; Yang, G.; Yang, Y.; Yu, L.; Wu, Y.; Li, G. *Nat. Photonics* **2009**, *3*, 649. (b) Dou, L.; You, J.; Yang, J.; Chen, C.-C.; He, Y.; Murase, S.; Moriarty, T.; Emery, K.; Li, G.; Yang, Y. *Nat. Photonics* **2012**, *6*, 180. (c) Sun, B.; Hong, W.; Yan, Z.; Aziz, H.; Li, Y. *Adv. Mater.* **2014**, *26*, 2636. (d) Zhang, C.; Zang, Y.; Gann, E.; McNeill, C. R.; Zhu, X.; Di, C.-a.; Zhu, D. *J. Am. Chem. Soc.* **2014**, *136*, 16176. (e) Gong, X.; Tong, M.; Xia, Y.; Cai, W.; Moon, J. S.; Cao, Y.; Yu, G.; Shieh, C.-L.; Nilsson, B.; Heeger, A. J. *Science* **2009**, *325*, 1665. (f) Meng, H.; Tucker, D.; Chaffins, S.; Chen, Y.; Helgeson, R.; Dunn, B.; Wudl, F. *Adv. Mater.* **2003**, *15*, 146. (g) Yao, Y.; Liang, Y.; Shrotriya, V.; Xiao, S.; Yu, L.; Yang, Y. *Adv. Mater.* **2007**, *19*, 3979. (h) Zhang, C.; Li, H.; Wang, J.; Zhang, Y.; Qiao, Y.; Huang, D.; Di, C.-a.; Zhan, X.; Zhu, X.; Zhu, D. *J. Mater. Chem. A* **2015**, *3*, 11194.
(5) Cava, M. P.; Lakshmikantham, M. V. *Acc. Chem. Res.* **1975**, *8*, 139.
(6) (a) Pomerantz, M.; Gu, X. *Synth. Met.* **1997**, *84*, 243. (b) Neef, C. J.; Brotherston, I. D.; Ferraris, J. P. *Chem. Mater.* **1999**, *11*, 1957. (c) Pomerantz, M.; Gu, X.; Zhang, S. *Macromolecules* **2001**, *34*, 1817. (d) Lee, K.; Sotzing, G. A. *Macromolecules* **2001**, *34*, 5746.
(7) (a) Liang, Y.; Yu, L. *Acc. Chem. Res.* **2010**, *43*, 1227. (b) Lu, L.; Yu, L. *Adv. Mater.* **2014**, *26*, 4413.
(8) Okuda, Y.; Lakshmikantham, M. V.; Cava, M. P. *J. Org. Chem.* **1991**, *56*, 6024.
(9) (a) Martin, R.; Diederich, F. *Angew. Chem., Int. Ed.* **1999**, *38*, 1350. (b) Gierschner, J.; Cornil, J.; Egelhaaf, H.-J.; Martin, R. E.; Diederich, F. *Adv. Mater.* **2007**, *19*, 173.
(10) (a) Casado, J.; Ponce Ortiz, R.; López Navarrete, J. T. *Chem. Soc. Rev.* **2012**, *41*, 5672. (b) Takahashi, T.; Matsuoka, K.; Takimiya, K.; Otsubo, T.; Aso, Y. *J. Am. Chem. Soc.* **2005**, *127*, 8928.
(11) Wencel-Delord, J.; Glorius, F. *Nat. Chem.* **2013**, *5*, 369.
(12) Izumi, T.; Kobashi, S.; Takimiya, K.; Aso, Y.; Otsubo, T. *J. Am. Chem. Soc.* **2003**, *125*, 5286.
(13) Meier, H.; Stalmach, U.; Kolshorn, H. *Acta Polym.* **1997**, *48*, 379.
(14) Becker, R. S.; de Melo, J. S.; Maçanita, A. L.; Elisei, F. *J. Phys. Chem.* **1996**, *100*, 18683.
(15) Lanzani, G.; Nisoli, M.; de Silvestri, S.; Turbino, R. *Chem. Phys. Lett.* **1996**, *251*, 339.
(16) (a) Casado, J.; Zgierski, M. Z.; Ewbank, P. C.; Burand, M. W.; Janzen, D. E.; Mann, K. R.; Rappenfus, T. M.; Berlin, A.; Casado, J.; Zgierski, M. Z.; Ewbank, P. C.; Buran, L. *J. Am. Chem. Soc.* **2006**, *128*, 10134. (b) Pina, J.; Burrows, H. D.; Becker, R. S.; Dias, F. B.; Macanita, A. L.; Seixas de Melo, J. *J. Phys. Chem. B* **2006**, *110*, 6499.
(17) Gidron, O.; Diskin-Posner, Y.; Bendikov, M. *J. Am. Chem. Soc.* **2010**, *132*, 2148.
(18) von Ragué Schleyer, Paul; Maerker, C.; Dransfeld, A.; Jiao, H.; van Eikema Hommes, N. J. R. *J. Am. Chem. Soc.* **1996**, *118*, 6317.
(19) Hotta, S.; Waragai, K. *J. Mater. Chem.* **1991**, *1*, 835.
(20) Castiglioni, C.; Tommasini, M.; Zerbi, G. *Philos. Trans. R. Soc., A* **2004**, *362*, 2425.
(21) Hernandez, V.; Casado, J.; Ramírez, F. J.; Zotti, G.; Hotta, S.; López Navarrete, J. T. *J. Chem. Phys.* **1996**, *104*, 9271.
(22) (a) Birnbaum, D.; Fichou, D.; Kohler, B. E. *J. Chem. Phys.* **1992**, *96*, 165. (b) *Handbook of Oligo- and Polythiophenes*; Fichou, D., Ed.; Wiley-VCH: Weinheim, 1999. (c) Wasserberg, D.; Meskers, S. C. J.; Janssen, R. A. J.; Mena-Osteritz, E.; Bäuerle, P. *J. Am. Chem. Soc.* **2006**, *128*, 17007. (d) Wasserberg, D.; Marsal, P.; Meskers, S. C. J.; Janssen, R. A. J.; Beljonne, D. *J. Phys. Chem. B* **2005**, *109*, 4410.
(23) (a) Bäuerle, P.; Segelbacher, U.; Maier, A.; Mehring, M. *J. Am. Chem. Soc.* **1993**, *115*, 10217. (b) van Haare, J. A. E. H.; Havinga, E. E.; van Dongen, J. L. J.; Janssen, R. A. J.; Cornil, J.; Brédas, J. L. *Chem. - Eur. J.* **1998**, *4*, 1509. (c) Casado, J.; Miller, L. L.; Mann, K. R.; Pappenfus, T. M.; Higuchi, H.; Orti, E.; Milian, B.; Pou-Amerigo, R.; Hernandez, V.; López Navarrete, J. T. *J. Am. Chem. Soc.* **2002**, *124*, 12380.
(24) (a) Furukawa, Y. *J. Phys. Chem.* **1996**, *100*, 15644. (b) Casado, J.; Miller, L. L.; Mann, K. R.; Pappenfus, T. M.; Hernández, V.; López Navarrete, J. T. *J. Phys. Chem. B* **2002**, *106*, 3597.
(25) Groenendaal, L.; Jonas, F.; Freitag, D.; Pielartzik, H.; Reynolds, J. R. *Adv. Mater.* **2000**, *12*, 481.
(26) Yang, J.-P.; Paa, W.; Rentsch, S. *Chem. Phys. Lett.* **2000**, *320*, 665.
(27) (a) Congreve, D. N.; Lee, J.; Thompson, N. J.; Hontz, E.; Yost, S. R. P.; Reusswig, D.; Bahlke, M. E.; Reineke, S.; van Woorhis, T.; Baldo, M. A. *Science* **2013**, *340*, 334. (b) Zimmerman, P. M.; Zhang, Z.; Musgrave, C. B. *Nat. Chem.* **2010**, *2*, 648. (c) Smith, M. B.; Michl, J. *Chem. Rev.* **2010**, *110*, 6891.
(28) (a) Minami, T.; Nakano, M. *J. Phys. Chem. Lett.* **2012**, *3*, 145. (b) Varnavski, O.; Abeyasinghe, N.; Aragó, J.; Serrano-Pérez, J. J.; Ortí, E.; Takimiya, K.; López Navarrete, J. T.; Casanova, D.; Casado, J.; Goodson, T. *J. Phys. Chem. Lett.* **2015**, *6*, 1375.
(29) Bange, S.; Scherf, U.; Lupton, J. M. *J. Am. Chem. Soc.* **2012**, *134*, 1946.
(30) (a) Brocklehurs, B. *J. Chem. Soc., Faraday Trans. 2* **1976**, *72*, 1869. (b) Burshtein, A. I.; Ivanov, K. L. *Phys. Chem. Chem. Phys.* **2002**, *4*, 4115.
(31) (a) *Handbook of Thiophene-Based Materials: Applications in Organic Electronics and Photonics*; Perepichka, D. F., Ed.; John Wiley & Sons: New York, 2009. (b) Fukazawa, A.; Kishi, D.; Tanaka, Y.; Seki, S.; Yamaguchi, S. *Angew. Chem., Int. Ed.* **2013**, *52*, 12091. (c) Mishra, A.; Ma, C.-Q.; Bäuerle, P. *Chem. Rev.* **2009**, *109*, 1141.
(32) Mames, A.; Stecko, S.; Mikozajczyk, P.; Soluch, M.; Furman, B.; Chmielewski, M. *J. Org. Chem.* **2010**, *75*, 7580.
(33) Bolstad, D. B.; Bolstad, E. S. S.; Frey, K. M.; Wright, D. L.; Anderson, A. C. *J. Med. Chem.* **2008**, *51*, 6839.
(34) Gronowitz, S.; Hallberg, A.; Glennow, C. *J. Heterocycl. Chem.* **1980**, *17*, 171.

DOI: 10.1021/jacs.5b05940
J. Am. Chem. Soc. 2015, 137, 10357−10366